Published in final edited form as:
Cell. 2012 February 3; 148(3): 556–567. doi:10.1016/j.cell.2011.11.062.

Fibroblast Growth Factor-21 Regulates PPARγ Activity and the Antidiabetic Actions of Thiazolidinediones

Paul A. Dutchak[1], **Takeshi Katafuchi**[2], **Angie L. Bookout**[2,3], **Jang Hyun Choi**[5], **Ruth T. Yu**[6], **David J. Mangelsdorf**[2,4], and **Steven A. Kliewer**[1,2]

[1]Department of Molecular Biology, University of Texas Southwestern Medical Center, Dallas, TX 75390-9041, USA

[2]Department of Pharmacology, University of Texas Southwestern Medical Center, Dallas, TX 75390-9041, USA

[3]Division of Hypothalamic Research, Department of Internal Medicine, University of Texas Southwestern Medical Center, Dallas, TX 75390-9041, USA

[4]Howard Hughes Medical Institute, University of Texas Southwestern Medical Center, Dallas, TX 75390-9041, USA

[5]Department of Cancer Biology and Division of Metabolism and Chronic Disease, Dana-Farber Cancer Institute and Department of Cell Biology, Harvard Medical School, Boston, Massachusetts 02115, USA

[6]Gene Expression Laboratory, Salk Institute for Biological Studies, La Jolla, California, USA

SUMMARY

Fibroblast growth factor-21 (FGF21) is a circulating hepatokine that beneficially affects carbohydrate and lipid metabolism. Here we report that FGF21 is also an inducible, fed-state autocrine factor in adipose tissue that functions in a feed-forward loop to regulate the activity of peroxisome proliferator-activated receptor γ (PPARγ), a master transcriptional regulator of adipogenesis. FGF21-knockout (KO) mice display defects in PPARγ signaling including decreased body fat and attenuation of PPARγ-dependent gene expression. Moreover, FGF21-KO mice are refractory to both the beneficial insulin-sensitizing effects and the detrimental weight gain and edema side effects of the PPARγ agonist rosiglitazone. This loss of function in FGF21-KO mice is coincident with a marked increase in the sumoylation of PPARγ, which reduces its transcriptional activity. Adding back FGF21 prevents sumoylation and restores PPARγ activity. Collectively, these results reveal FGF21 as a key mediator of the physiologic and pharmacologic actions of PPARγ.

Corresponding authors: David J. Mangelsdorf (davo.mango@utsouthwestern.edu) and Steven A. Kliewer (steven.kliewer@utsouthwestern.edu).

SUPPLEMENTAL INFORMATION

Supplemental information, including four figures and supplemental experimental procedures, can be found with this article online.

INTRODUCTION

While white adipose tissue (WAT) serves as a repository for fatty acids, it also plays a crucial role in regulating overall energy homeostasis (Spiegelman and Flier, 2001). Either too little or too much WAT contributes to metabolic abnormalities that include hyperlipidemia, insulin resistance and type 2 diabetes. Thus, maintaining the appropriate amount of WAT is crucial for optimal health.

Peroxisome proliferator-activated receptor γ (PPARγ) is a member of the nuclear receptor family of ligand-activated transcription factors that is highly expressed in WAT (Chawla et al., 1994; Tontonoz et al., 1994a), where it is required for adipocyte differentiation (Rosen et al., 1999; Tontonoz et al., 1994b). PPARγ exists as two isoforms, PPARγ1 and PPARγ2, with PPARγ2 containing an additional 30 amino acids at its amino terminus (Tontonoz et al., 1994a). PPARγ cooperates with the CCAAT/enhancer-binding protein (C/EBP) family of transcription factors to regulate adipogenesis. C/EBPβ and C/EBPδ are present early during adipogenesis and induce PPARγ expression (Cao et al., 1991; Wu et al., 1996; Wu et al., 1999; Wu et al., 1995; Yeh et al., 1995). C/EBPα is expressed later and together with PPARγ governs the adipocyte-specific pattern of gene expression (Lefterova et al., 2008; Tontonoz et al., 1994b; Wu et al., 1998). While the identity of the endogenous PPARγ ligand is unknown, PPARγ is activated by various fatty acids and fatty acid metabolites as well as by the thiazolidinedione (TZD) class of insulin-sensitizing drugs, which include rosiglitazone and pioglitazone (Tontonoz and Spiegelman, 2008; Willson et al., 2001). PPARγ activity is also regulated by post-translational modification, including phosphorylation and sumoylation. Phosphorylation of PPARγ2 at S112 by MAP kinases represses its transcriptional activity by inhibiting ligand binding and altering cofactor recruitment (Adams et al., 1997; Hu et al., 1996; Shao et al., 1998). Phosphorylation of PPARγ2 at S273 by CDK5 does not alter its adipogenic capacity but dysregulates numerous genes involved in obesity (Choi et al., 2010). Sumoylation of PPARγ2 at K107 blocks its transcriptional activity (Floyd and Stephens, 2004; Ohshima et al., 2004; Yamashita et al., 2004), possibly by promoting corepressor recruitment. In macrophages, sumoylation of PPARγ2 at K395 results in its recruitment to the promoters of inflammatory genes, where it inhibits transcription by preventing clearance of corepressor complexes (Pascual et al., 2005).

Fibroblast growth factor-21 (FGF21) is an atypical member of the FGF family that functions as a hormone to regulate carbohydrate and lipid metabolism. FGF21 was first shown to regulate metabolism in 3T3-L1 adipocytes, where it stimulated glucose uptake (Kharitonenkov et al., 2005). When administered pharmacologically to obese, insulin resistant rodents and monkeys, FGF21 increased energy expenditure, insulin sensitivity and weight loss and normalized carbohydrate and lipid parameters (Berglund et al., 2009; Coskun et al., 2008; Kharitonenkov et al., 2005; Kharitonenkov et al., 2007; Xu et al., 2009). FGF21 is strongly induced in liver in response to fasting or ketogenic diet (Badman et al., 2007; Inagaki et al., 2007; Lundasen et al., 2007). Consistent with a role in the adaptive fasting response, FGF21 stimulated hepatic ketogenesis and gluconeogenesis in lean mice (Potthoff et al., 2009), and FGF21-transgenic mice were growth inhibited and sensitized to the hibernation-like state of torpor (Inagaki et al., 2007; Inagaki et al., 2008). Mechanistically, FGF21 activates cell signaling by binding to a heteromeric cell surface receptor tyrosine kinase complex composed of β-Klotho and a conventional FGF receptor (FGFR), with FGFR1c being the preferred isoform for FGF21 (Ogawa et al., 2007; Suzuki et al., 2008). Both β-Klotho and FGFR1c are abundantly expressed in WAT (Fon Tacer et al., 2010; Kurosu et al., 2007), where FGF21-regulated genes are involved in a variety of metabolic processes including lipogenesis, lipolysis and fatty acid oxidation (Coskun et al.,

2008; Xu et al., 2009). Based upon these findings, it was proposed that FGF21 induces futile cycling and energy expenditure in WAT (Coskun et al., 2008).

During fasting, FGF21 expression in liver is controlled by PPARα, and pharmacologic administration of PPARα agonists (e.g., the fibrate class of hypolipidemic drugs) induces hepatic expression of FGF21 (Badman et al., 2007; Inagaki et al., 2007; Lundasen et al., 2007). However, FGF21 is also induced by PPARγ agonists, including TZDs, in WAT and isolated adipocytes (Muise et al., 2008; Wang et al., 2008; Zhang et al., 2008). While FGF21 and rosiglitazone were shown to cooperate in promoting differentiation and glucose uptake in 3T3-L1 adipocytes (Moyers et al., 2007), the functional relationship between TZDs and FGF21 has not been explored in vivo. Here, we show that FGF21 acts in an autocrine fashion in WAT to regulate PPARγ activity, to enhance adipogenesis and to contribute to both the therapeutic and side effects of TZDs. These studies reveal a previously unrecognized facet of FGF21 biology.

RESULTS

FGF21 is induced in WAT by feeding

A previous study showed that *Fgf21* is induced by rosiglitazone in WAT of wild-type and *db/db* mice (Muise et al., 2008). Consistent with these findings, FGF21 mRNA and protein levels were induced by rosiglitazone in WAT but not liver of wild-type mice (Figures 1A–1D). Conversely, FGF21 mRNA and protein concentrations were increased by the PPARα agonist, GW7647, in liver but not WAT (Figures 1A–1D). Notably, whereas GW7647 markedly increased plasma FGF21 concentrations, rosiglitazone had no effect (Figure 1E). In experiments performed with isolated adipocytes, rosiglitazone but not GW7647 increased both FGF21 mRNA levels and protein concentrations in the media (Figure S1). Taken together, these data suggest that FGF21 is secreted from WAT but acts locally in an autocrine or paracrine fashion instead of entering the circulation.

To determine whether *Fgf21* is induced in WAT by diet, *Fgf21* mRNA levels were measured at 4 hour intervals in WAT and liver from mice restricted to feeding during a 4 hour period in the middle of the dark cycle. As expected, *Fgf21* expression was highest in liver just prior to feeding (Figure 1F). In contrast, *Fgf21* expression in WAT was very low during fasting but spiked 4 hours after feeding to an absolute level comparable to that seen in liver of fasted mice (Figure 1F). Thus, *Fgf21* is induced in WAT by either TZD treatment or feeding. Under these conditions, we saw no significant changes in the levels of circulating FGF21 (data not shown), which is consistent with increases in blood FGF21 concentrations requiring fasting for 24 hours or more (Muise et al., 2008).

FGF21-knockout (KO) mice have mild lipodystrophy

Given the regulation of *Fgf21* in WAT, we examined whether FGF21-KO mice have an adipose tissue phenotype. While FGF21-KO mice had no change in body mass or fluid mass, they had a significant decrease in total fat mass and a significant increase in lean mass (Figures 2A–2D). There was no difference in food intake between wild-type and FGF21-KO mice (data not shown). Consistent with these findings, FGF21-KO mice had significantly reduced amounts of epididymal, subcutaneous, mesenteric, retroperitoneal and interscapular brown adipose tissue (BAT) (Figure 2E). There was no difference in the DNA content of epididymal WAT from wild-type and FGF21-KO mice (Figure 2F), indicating that the decreased adiposity was a consequence of smaller adipocytes rather than a decrease in adipocyte number. This difference in adipocyte size was confirmed by histomorphometry (Figures 2G and 2H). Similar effects on fat mass, lean mass and epididymal, subcutaneous and retroperitoneal adipose depot mass were seen in FGF21-KO mice crossed into the

C57Bl/6 background (Figures S2A–S2E). We note that two other groups reported increased adiposity in FGF21-KO mice (Badman et al., 2009; Hotta et al., 2009). A possible explanation for this discrepancy is that the diets used by these groups contained soy whereas ours did not.

FGF21 enhances adipocyte differentiation

To determine whether the adipose tissue phenotype was cell autonomous, we examined the differentiation of preadipocytes derived from wild-type and FGF21-KO mice. *Fgf21* mRNA levels were low but detectable in wild-type preadipocytes prior to differentiation (Figure 3A). *Fgf21* expression decreased during the first day of differentiation but then rose steadily over the 8 day differentiation protocol. The mRNA encoding β-Klotho (*Klb*), an essential component of the FGF21 receptor (Ogawa et al., 2007; Suzuki et al., 2008), was virtually undetectable until day 4 of differentiation and then rose throughout the differentiation period (Figure 3A). Interestingly, *Klb* mRNA levels were lower in FGF21-KO adipocytes but restored by inclusion of recombinant FGF21 in the differentiation medium (Figure 3A). Expression of *Fgfr1c*, which encodes the other subunit of the FGF21 receptor, decreased during the early stages of differentiation and was unaffected by the absence of FGF21 (Figure 3A). These data suggest that FGF21 signaling initiates between days 2 and 4 of adipocyte differentiation.

We next examined the temporal pattern of expression for a panel of genes that are expressed during the differentiation process. The expression pattern for *Cebpb* and *Cebpd*, which play important roles in the early stages of adipocyte differentiation (Cao et al., 1991; Wu et al., 1999; Yeh et al., 1995), was similar between wild-type and FGF21-KO adipocytes and unaffected by treatment with recombinant FGF21 (Figure 3A). In contrast, the induction of *Cebpa* and *Pparg* mRNAs was delayed in FGF21-KO adipocytes. Whereas *Pparg* expression was efficiently restored by recombinant FGF21, *Cebpa* expression was not (Figure 3A). The mRNAs encoding the fatty acid binding protein, *ap2*, and the lipogenic proteins solute carrier family 25, member 1 (*Slc25a1*), ATP citrate lyase (*Acly*), malic enzyme (*Me1*), acetyl-CoA carboxylase α (*Acaca*), fatty acid synthase (*Fasn*), and diacylglycerol O-acyltransferase 2 (*Dgat2*) had similar expression patterns: the level of each was reduced in FGF21-KO adipocytes and at least partially restored by treatment with recombinant FGF21 (Figure 3A). For *Cebpa*, *Pparg* and most of the lipogenic genes, reduced expression was first observed at day 4 of differentiation, consistent with when *Klb* mRNA first appears in wild-type adipocytes (Figure 3A). Phosphoenolpyruvate carboxykinase (*Pck1*), which was induced only at day 8 of differentiation, was also reduced in FGF21-KO adipocytes and partially restored by recombinant FGF21 (Figure 3A). In agreement with the lipogenic gene expression data, lipid accumulation was reduced in FGF21-KO adipocytes and restored to wild-type levels in the presence of recombinant FGF21 (Figure 3B).

FGF21 stimulates PPARγ transcriptional activity

The impaired differentiation and lipid accumulation in FGF21-KO adipocytes suggested that FGF21 might regulate PPARγ activity. To examine this, wild-type and FGF21-KO adipocytes were differentiated in the presence or absence of rosiglitazone. As expected, rosiglitazone treatment increased lipogenic gene expression and lipid accumulation in wild-type adipocytes (Figures 4A and 4B). However, the stimulatory effects of rosiglitazone were attenuated in FGF21-KO adipocytes. Inclusion of recombinant FGF21 rescued the effect of rosiglitazone on gene expression and lipid accumulation in the FGF21-KO adipocytes (Figures 4A and 4B).

Total PPARγ protein levels were unchanged in primary adipocytes either lacking endogenous FGF21 or treated with recombinant FGF21 (Figure 4C). Likewise, there was no

change in the level of PPARγ phosphorylated at S112 under these conditions (Figure S3A). Notably, however, there was a significant increase in sumoylated PPARγ in FGF21-KO adipocytes (Figure 4C). This increase in PPARγ sumoylation was reversed by including recombinant FGF21 in the media (Figure 4C). In agreement with these in vitro results, there was a significant increase in PPARγ sumoylation in WAT from FGF21-KO mice (Figure 4D) and a corresponding decrease in PPARγ target gene expression (Figure 4E). There was no change in PPARγ phosphorylation at either S112 or S273 in WAT from FGF21-KO mice (Figures S3A and S3B). Similar effects on PPARγ sumoylation and target gene expression were seen in FGF21-KO mice crossed onto the C57Bl/6 background (Figures S3C and S3D). Taken together, the in vitro and in vivo data suggest that FGF21 increases PPARγ transcriptional activity by suppressing its sumoylation.

PPARγ can be sumoylated at K107 and K395 with different transcriptional outcomes (Floyd and Stephens, 2004; Ohshima et al., 2004; Pascual et al., 2005; Yamashita et al., 2004). To determine at which position PPARγ is sumoylated in FGF21-KO adipocytes, the sumoylation sites were mutated either singly or together in the context of a 3xFlag-tagged PPARγ, and the tagged PPARγ mutants introduced into FGF21-KO adipocytes. Mutating K107 (K107R) but not K395 (K395R) blocked PPARγ sumoylation as measured by immunoprecipitation with a Flag antibody followed by western blot analysis for the ~80 kD sumoylated PPARγ protein with either SUMO1 or PPARγ antibodies (Figures 4F and S3E). Sumoylation at K107 inhibits PPARγ activity (Floyd and Stephens, 2004; Ohshima et al., 2004; Yamashita et al., 2004). Thus, these data suggest that in the absence of FGF21, PPARγ transcriptional activity is impaired by sumoylation at K107.

We investigated whether introduction of the PPARγ-K107R sumoylation mutant into FGF21-KO pre-adipocytes would reverse their impaired differentiation phenotype. PPARγ-K395R was also included in these experiments as a control. Preadipocytes derived from wild-type and FGF21-KO mice were infected with lentiviruses expressing either wild-type PPARγ, the K107R or K395R sumoylation mutants or a control GFP-expressing virus. As expected, adipocytes from FGF21-KO mice infected with control (GFP) lentivirus showed decreased expression of *Slc25a1*, *Acly*, *Me1*, *Acaca*, *Fasn*, *Dgat2* and *Pck1* at the end of the differentiation period compared to adipocytes from wild-type mice (Figure 4G). Expression of these genes was rescued in FGF21-KO adipocytes by PPARγ-K107R but not wild-type PPARγ or PPARγ-K395R (Figure 4G). These data indicate that increased sumoylation of PPARγ in FGF21-KO adipocytes contributes to their altered phenotype.

FGF21-KO mice are refractory to rosiglitazone

If FGF21 is required for full PPARγ activity, then FGF21-KO mice should be resistant to the actions of TZDs. To test this prediction, groups of diet-induced obese (DIO) wild-type and FGF21-KO mice were treated with rosiglitazone or vehicle for 14 days. As expected, rosiglitazone induced FGF21 mRNA and protein in WAT of wild-type mice (Figures 5A and 5B). In contrast, rosiglitazone treatment decreased hepatic *Fgf21* mRNA levels and had little or no effect on hepatic FGF21 protein levels (Figures 5C and 5D). Circulating FGF21 concentrations were decreased by rosiglitazone treatment (Figure 5E). These data provide further evidence that FGF21 synthesized in WAT acts in an autocrine or paracrine manner rather than circulating as a hormone.

As expected, rosiglitazone treatment significantly reduced plasma glucose and insulin concentrations in wild-type mice (Figure 5F). While plasma insulin and glucose levels trended lower in rosiglitazone-treated FGF21-KO mice, these differences were not statistically significant (Figure 5F). Importantly, rosiglitazone treatment improved glucose disposal in glucose and insulin tolerance tests in wild-type but not FGF21-KO mice (Figures 5G and 5H). In glucose tolerance tests, rosiglitazone decreased plasma insulin

concentrations in both wild-type and FGF21-KO mice (Figure 5I). This result was surprising in the FGF21-KO mice given the lack of an effect of rosiglitazone treatment on glucose concentrations. Notably, peak insulin concentrations were significantly higher in wild-type mice compared to FGF21-KO mice (Figure 5I), suggesting that FGF21-KO mice have impaired insulin secretion. This is consistent with the finding that FGF21 stimulated insulin secretion in isolated rodent islets (Wente et al., 2006). Plasma non-esterified fatty acid and triglyceride concentrations and hepatic triglyceride concentrations were either significantly increased or trended upward in FGF21-KO mice compared to wild-type mice (Figures 5J–5L). Rosiglitazone decreased these parameters in FGF21-KO mice to levels comparable to those in rosiglitazone-treated wild-type mice. We conclude that FGF21 is required for some but not all of the metabolic effects of rosiglitazone in DIO mice. We further conclude that some of these effects are likely to involve FGF21 acting on tissues other than WAT, including pancreas.

Two well-established side effects of TZDs are increased adiposity and fluid retention. While rosiglitazone did not significantly change body mass in DIO wild-type or FGF21-KO mice, it significantly increased fat mass and fluid mass and decreased lean mass in wild-type mice (Figures 5M–5P). Notably, the effects of rosiglitazone on fat mass, lean mass and fluid mass were absent in FGF21-KO mice (Figures 5N–5P). Thus, FGF21 is required for both beneficial and adverse effects of rosiglitazone.

We next compared WAT from DIO wild-type and FGF21-KO mice treated with rosiglitazone or vehicle. Phosphorylation of Akt at S473 in WAT was higher in wild-type mice than FGF21-KO mice after treatment with either rosiglitazone or rosiglitazone plus insulin (Figure S4), indicating that the absence of FGF21 impairs insulin sensitivity in adipose. As expected, rosiglitazone treatment decreased adipocyte size in wild-type mice (Figure 6A). Interestingly, under DIO conditions, adipocytes were larger in FGF21-KO mice. Furthermore, in DIO FGF21-KO mice, rosiglitazone treatment was less effective at decreasing adipocyte size and consequently the adipocytes remained significantly larger than those from wild-type mice treated with rosiglitazone (Figure 6A). As was observed in chow fed mice, sumoylated PPARγ levels in WAT were markedly increased in DIO FGF21-KO mice compared to wild-type mice (Figure 6B). Consistent with these findings, microarray analysis revealed large clusters of genes that were either up-regulated or down-regulated in response to rosiglitazone treatment in wild-type mice but not in FGF21-KO mice (Figure 6C). Loss of rosiglitazone responsiveness in FGF21-KO WAT was confirmed for a subset of PPARγ target genes by RT-qPCR (Figure 6D). For reasons that are not known, basal expression of *Slc25a1* and *Fasn* was elevated in WAT of FGF21-KO mice (Figure 6D). *Pck1* expression was significantly reduced in FGF21-KO WAT and unresponsive to rosiglitazone treatment (Figure 6D). Analysis of adipokines revealed the expected decrease in *Tnfa* expression in WAT of wild-type mice treated with rosiglitazone (Figure 6E). This response was absent in FGF21-KO mice (Figure 6E). While plasma adiponectin levels increased in response to rosiglitazone administration in both wild-type and FGF21-KO mice, this induction was significantly attenuated in FGF21-KO mice (Figure 6F). Taken together, these data show that the actions of rosiglitazone are compromised in DIO FGF21-KO mice.

DISCUSSION

In this report we demonstrate an important role for FGF21 in regulating PPARγ activity in WAT. FGF21 was previously shown to be induced by PPARγ agonists in WAT and to cooperate with rosiglitazone in promoting differentiation and glucose uptake in 3T3-L1 adipocytes in vitro (Moyers et al., 2007; Muise et al., 2008; Wang et al., 2008; Zhang et al., 2008). We now show that lean mice lacking FGF21 have decreased PPARγ activity in

WAT and corresponding reductions in WAT mass and adipocyte size. We further show that obese, insulin resistant mice lacking FGF21 are refractory to the actions of rosiglitazone, including both beneficial and adverse effects. We conclude that the actions of FGF21 and PPARγ are fundamentally intertwined in WAT.

A surprising result from our studies is that rosiglitazone-mediated induction of FGF21 in WAT does not cause a corresponding increase in circulating FGF21 in either lean or DIO mice. In DIO mice, plasma FGF21 levels decreased in parallel with reduced *Fgf21* mRNA in liver. In agreement with a previous study (Zhang et al., 2008), we show that rosiglitazone treatment of isolated adipocytes increased FGF21 in the media, demonstrating that FGF21 is secreted from adipocytes in vitro. A parsimonious explanation for these data is that FGF21 is secreted from adipocytes but is unable to reach the circulation, perhaps due to interactions with the WAT extracellular matrix. Thus, FGF21 is restricted to acting in an autocrine or paracrine manner in WAT, much like conventional FGFs. FGF21 is also proposed to act through an autocrine mechanism in exocrine pancreas and liver (Fisher et al., 2010; Johnson et al., 2009). In recent human studies, rosiglitazone treatment had no effect on circulating FGF21 concentrations in subjects who were either healthy or had impaired glucose tolerance (Christodoulides et al., 2009; Mai et al., 2009), but significantly decreased circulating FGF21 in patients with type 2 diabetes (Li et al., 2009a). This latter study together with the finding that rosiglitazone induces FGF21 expression in primary cultures of human adipocytes (Zhang et al., 2008) suggest that FGF21 is regulated similarly in mice and man. However, while one group reported that *Fgf21* mRNA is present in human WAT (Zhang et al., 2008), another group detected little or no *Fgf21* mRNA in human WAT samples (Dushay et al., 2010). Additional studies will be required to determine the relevance of FGF21 expression in human WAT in both physiologic and pharmacologic contexts.

Previous studies showed that sumoylation of PPARγ at K107 represses its transcriptional activity in vitro (Floyd and Stephens, 2004; Ohshima et al., 2004; Yamashita et al., 2004). However, the in vivo relevance of this PPARγ sumoylation event remained unclear. We now show that the absence of FGF21 causes a marked increase in sumoylated PPARγ in WAT in vivo. This increase in sumoylated PPARγ corresponds to a decrease in the expression of PPARγ target genes. Our in vitro studies with FGF21-KO adipocytes show that PPARγ sumoylation occurs at K107. We further show that the effect of FGF21 deficiency on adipocyte differentiation can be overcome by expressing a PPARγ K107 mutant, strongly suggesting that increased PPARγ sumoylation contributes to the FGF21-KO phenotype. Precisely how sumoylation blocks the transcriptional activity of PPARγ remains unclear, although in vitro studies suggest that it may involve the recruitment of corepressor proteins (Yamashita et al., 2004). Notably, sumoylation of PPARγ is reduced by mutating the adjacent phosphorylation site at S112 (Yamashita et al., 2004), which also increases PPARγ transcriptional activity (Adams et al., 1997; Hu et al., 1996; Shao et al., 1998). However, we did not see increased PPARγ S112 phosphorylation in FGF21-KO WAT, suggesting that phosphorylation and sumoylation are not coupled in this context.

Based on the data in sum, we propose a feed-forward regulatory model wherein PPARγ induces FGF21 in WAT, which then acts in an autocrine or paracrine manner to block PPARγ sumoylation (Figure 6G). The net effect is an increase in PPARγ activity in mid- to late-stage pre-adipocytes and mature adipocytes, which express both β-Klotho and FGFR1c. We further propose that FGF21 contributes to the antidiabetic TZD response in adipose tissue through at least two PPARγ-dependent mechanisms: by increasing the number of small, metabolically active adipocytes and by raising adiponectin levels in the circulation. While DIO FGF21-KO mice were refractory to rosiglitazone treatment, we note that the drug response was not eliminated. Rosiglitazone still significantly decreased plasma and

hepatic triglyceride concentrations and decreased plasma insulin concentrations in glucose tolerance tests in FGF21-KO mice. Thus, rosiglitazone has FGF21-independent effects.

Our finding that FGF21 is required for rosiglitazone to increase adiposity and fluid mass is puzzling for two reasons. First, while the adiposity findings are consistent with FGF21 expression and induction by TZDs in WAT, they appear at odds with pharmacologic studies in which exogenous FGF21 administration causes significant weight loss in obese animals (Kharitonenkov et al., 2005; Kharitonenkov et al., 2007). We suggest that this may reflect the difference between endogenous FGF21 acting in a paracrine fashion on WAT alone versus exogenous FGF21 acting coordinately on multiple tissues including liver, where FGF21 stimulates fatty acid oxidation and ketogenesis (Badman et al., 2007; Inagaki et al., 2007; Potthoff et al., 2009), BAT, where FGF21 increases thermogenesis (Hondares et al., 2010), and the central nervous system, where FGF21 enhances insulin sensitivity (Sarruf et al., 2010). Thus, pharmacologic administration of FGF21 may provide a means of obtaining the beneficial, insulin-sensitizing effects of PPARγ agonists without causing weight gain. A second puzzle is how the absence of FGF21 influences TZD-mediated increases in fluid mass since neither FGF21 nor its co-receptor, β-Klotho, appear to be expressed in the kidney (Fon Tacer et al., 2010), where activation of PPARγ decreases urinary sodium excretion and increases fluid retention (Guan et al., 2005; Zhang et al., 2005). However, we note that the effects of TZDs on fluid retention are not entirely eliminated by removing PPARγ in kidney (Zhang et al., 2005), suggesting that other tissues are involved. It remains to be determined how FGF21 impacts TZD-mediated changes in fluid mass.

Why might a hormone that elicits diverse aspects of the starvation response — presumably by acting on multiple tissues — be selectively induced in WAT in the fed state? One possibility is that FGF21 regulates pathways in WAT that are important under both fed and fasted conditions. A notable example of this is triglyceride synthesis. In the fed state, glucose and fatty acids are stored as triglyceride in WAT. However, triglyceride synthesis also plays an important role during fasting, when ~75% of fatty acids released by lipolysis are reabsorbed and re-esterified by WAT and other tissues, including liver (Reshef et al., 2003). This “triglyceride/fatty acid cycle” is believed to serve as a mechanism for controlling the delivery of substrates to tissues, including fatty acids and glycerol to the liver for ketogenesis and gluconeogenesis, respectively (Reshef et al., 2003). Our finding that FGF21 regulates genes such as *Dgat2* and *Pck1* is consistent with the notion that it modulates triglyceride homeostasis in both the fed and fasted states. A role for FGF21 in controlling the triglyceride/fatty acid cycle may also explain why FGF21 has alternately been reported to stimulate (Inagaki et al., 2007) or to repress lipolysis in white adipocytes (Arner et al., 2008; Li et al., 2009b). While on the one hand FGF21 induces lipases such as adipose triglyceride lipase and hormone sensitive lipase that are involved in triglyceride hydrolysis and mobilization (Coskun et al., 2008; Inagaki et al., 2007), it also induces genes that are involved in triglyceride synthesis. Thus, the net effect of FGF21 on fatty acid homeostasis likely depends on the precise physiologic context. A role for FGF21 in modulating the triglyceride/fatty acid cycle is consistent with the elevated circulating fatty acid levels that occur in FGF21-KO mice during fasting (Hotta et al., 2009; Potthoff et al., 2009).

In summary, we describe an unexpected role for FGF21 in white adipocytes. We conclude that FGF21 has two, disparate physiologic functions: as an endocrine hormone secreted by the liver to coordinate the adaptive response during starvation; and, as an autocrine or paracrine factor induced in WAT during the fed state to regulate adipocyte function.

EXPERIMENTAL PROCEDURES

Animal Experiments

FGF21-KO mice were generated as described (Potthoff et al., 2009), including two generations of heterozygous crosses, and maintained on a mixed C57Bl/6 × 129 genetic background as separate wild-type (*Fgf21*$^{+/+}$) and homozygous knockout (*Fgf21*$^{-/-}$) breeding lines. For pure strain studies, FGF21-KO mice were backcrossed for six generations onto the C57Bl/6 background. Mice were maintained on a standard chow diet containing 4% fat (Harlan Teklad Global Diet #2916). All experiments were performed with male mice. DIO mice were fed a high fat diet containing 60% kcal from fat (Research Diets Inc. #D12492). Oral glucose tolerance tests were performed on groups of DIO mice treated with rosiglitazone or vehicle for 1 week. One week later, after being maintained on the high fat and rosiglitazone regimen, insulin tolerance tests were performed on these same groups of mice. All animal experiments were approved by the Institutional Animal Research Advisory Committee of the University of Texas Southwestern Medical Center at Dallas.

Body Composition Analysis

Body composition was measured using a Bruker Minispec mq10 NMR.

Primary Adipocyte Differentiation Assays

Primary preadipocytes were isolated from P4 wild-type and FGF21-KO mice, grown to confluency and differentiated in media containing high glucose DMEM plus 10% FBS, 10 μg/ml insulin, 0.5 mM isobutylmethyxanthine and 0.25 μM dexamethasone.

Microarray Analysis

RNA prepared from epididymal WAT from DIO wild-type and FGF21-KO mice treated with rosiglitazone or vehicle for 14 days was reverse transcribed into cRNA, biotin-UTP labeled and hybridized to the Illumina mouseRefseq-8v2 Expression BeadChip.

Statistical Analysis

Statistical analyses were performed using Microsoft Excel 2007. Comparisons of two groups were performed using Student's t test. $p < 0.05$ was considered significant.

Supplementary Material

Refer to Web version on PubMed Central for supplementary material.

Acknowledgments

We thank Drs. Regina Goetz and Moosa Mohammadi for recombinant FGF21 protein, Dr. James Richardson for histopathology expertise and members of the Mangelsdorf/Kliewer laboratory for discussion. This research was supported by the Howard Hughes Medical Institute (D.J.M.), NIH grants RL1GM084436 and R56DK089600 (D.J.M. and S.A.K.), U19DK62434 (D.J.M), and GM007062 (A.L.B.), the Robert A. Welch Foundation (I-1275 to D.J.M. and I-1558 to S.A.K.) and the Leona M. and Harry B. Helmsley Charitable Trust (R.T.Y.).

References

Adams M, Reginato MJ, Shao D, Lazar MA, Chatterjee VK. Transcriptional activation by peroxisome proliferator-activated receptor gamma is inhibited by phosphorylation at a consensus mitogen-activated protein kinase site. J Biol Chem. 1997; 272:5128–5132. [PubMed: 9030579]

Arner P, Pettersson A, Mitchell PJ, Dunbar JD, Kharitonenkov A, Ryden M. FGF21 attenuates lipolysis in human adipocytes - a possible link to improved insulin sensitivity. FEBS Lett. 2008; 582:1725–1730. [PubMed: 18460341]

Badman MK, Koester A, Flier JS, Kharitonenkov A, Maratos-Flier E. Fibroblast growth factor 21-deficient mice demonstrate impaired adaptation to ketosis. Endocrinology. 2009; 150:4931–4940. [PubMed: 19819944]

Badman MK, Pissios P, Kennedy AR, Koukos G, Flier JS, Maratos-Flier E. Hepatic fibroblast growth factor 21 is regulated by PPARalpha and is a key mediator of hepatic lipid metabolism in ketotic states. Cell Metab. 2007; 5:426–437. [PubMed: 17550778]

Berglund ED, Li CY, Bina HA, Lynes SE, Michael MD, Shanafelt AB, Kharitonenkov A, Wasserman DH. Fibroblast growth factor 21 controls glycemia via regulation of hepatic glucose flux and insulin sensitivity. Endocrinology. 2009; 150:4084–4093. [PubMed: 19470704]

Cao Z, Umek RM, McKnight SL. Regulated expression of three C/EBP isoforms during adipose conversion of 3T3-L1 cells. Genes Dev. 1991; 5:1538–1552. [PubMed: 1840554]

Chawla A, Schwarz EJ, Dimaculangan DD, Lazar MA. Peroxisome proliferator-activated receptor (PPAR) gamma: adipose-predominant expression and induction early in adipocyte differentiation. Endocrinology. 1994; 135:798–800. [PubMed: 8033830]

Choi JH, Banks AS, Estall JL, Kajimura S, Bostrom P, Laznik D, Ruas JL, Chalmers MJ, Kamenecka TM, Bluher M, Griffin PR, Spiegelman BM. Anti-diabetic drugs inhibit obesity-linked phosphorylation of PPARgamma by Cdk5. Nature. 2010; 466:451–456. [PubMed: 20651683]

Christodoulides C, Dyson P, Sprecher D, Tsintzas K, Karpe F. Circulating fibroblast growth factor 21 is induced by peroxisome proliferator-activated receptor agonists but not ketosis in man. J Clin Endocrinol Metab. 2009; 94:3594–3601. [PubMed: 19531592]

Coskun T, Bina HA, Schneider MA, Dunbar JD, Hu CC, Chen Y, Moller DE, Kharitonenkov A. Fibroblast growth factor 21 corrects obesity in mice. Endocrinology. 2008; 149:6018–6027. [PubMed: 18687777]

Dushay J, Chui PC, Gopalakrishnan GS, Varela-Rey M, Crawley M, Fisher FM, Badman MK, Martinez-Chantar ML, Maratos-Flier E. Increased fibroblast growth factor 21 in obesity and nonalcoholic fatty liver disease. Gastroenterology. 2010; 139:456–463. [PubMed: 20451522]

Fisher FM, Chui PC, Antonellis PJ, Bina HA, Kharitonenkov A, Flier JS, Maratos-Flier E. Obesity is a fibroblast growth factor 21 (FGF21)-resistant state. Diabetes. 2010; 59:2781–2789. [PubMed: 20682689]

Floyd ZE, Stephens JM. Control of peroxisome proliferator-activated receptor gamma2 stability and activity by SUMOylation. Obes Res. 2004; 12:921–928. [PubMed: 15229330]

Fon Tacer K, Bookout AL, Ding X, Kurosu H, John GB, Wang L, Goetz R, Mohammadi M, Kuro-o M, Mangelsdorf DJ, Kliewer SA. Research resource: Comprehensive expression atlas of the fibroblast growth factor system in adult mouse. Mol Endocrinol. 2010; 24:2050–2064. [PubMed: 20667984]

Guan Y, Hao C, Cha DR, Rao R, Lu W, Kohan DE, Magnuson MA, Redha R, Zhang Y, Breyer MD. Thiazolidinediones expand body fluid volume through PPARgamma stimulation of ENaC-mediated renal salt absorption. Nat Med. 2005; 11:861–866. [PubMed: 16007095]

Hondares E, Rosell M, Gonzalez FJ, Giralt M, Iglesias R, Villarroya F. Hepatic FGF21 expression is induced at birth via PPARalpha in response to milk intake and contributes to thermogenic activation of neonatal brown fat. Cell Metab. 2010; 11:206–212. [PubMed: 20197053]

Hotta Y, Nakamura H, Konishi M, Murata Y, Takagi H, Matsumura S, Inoue K, Fushiki T, Itoh N. Fibroblast growth factor 21 regulates lipolysis in white adipose tissue but is not required for ketogenesis and triglyceride clearance in liver. Endocrinology. 2009; 150:4625–4633. [PubMed: 19589869]

Hu E, Kim JB, Sarraf P, Spiegelman BM. Inhibition of adipogenesis through MAP kinase-mediated phosphorylation of PPARgamma. Science. 1996; 274:2100–2103. [PubMed: 8953045]

Inagaki T, Dutchak P, Zhao G, Ding X, Gautron L, Parameswara V, Li Y, Goetz R, Mohammadi M, Esser V, Elmquist JK, Gerard RD, Burgess SC, Hammer RE, Mangelsdorf DJ, Kliewer SA. Endocrine regulation of the fasting response by PPARalpha-mediated induction of fibroblast growth factor 21. Cell Metab. 2007; 5:415–425. [PubMed: 17550777]

Inagaki T, Lin VY, Goetz R, Mohammadi M, Mangelsdorf DJ, Kliewer SA. Inhibition of growth hormone signaling by the fasting-induced hormone FGF21. Cell Metab. 2008; 8:77–83. [PubMed: 18585098]

Johnson CL, Weston JY, Chadi SA, Fazio EN, Huff MW, Kharitonenkov A, Koester A, Pin CL. Fibroblast growth factor 21 reduces the severity of cerulein-induced pancreatitis in mice. Gastroenterology. 2009; 137:1795–1804. [PubMed: 19664632]

Kharitonenkov A, Shiyanova TL, Koester A, Ford AM, Micanovic R, Galbreath EJ, Sandusky GE, Hammond LJ, Moyers JS, Owens RA, Gromada J, Brozinick JT, Hawkins ED, Wroblewski VJ, Li DS, Mehrbod F, Jaskunas SR, Shanafelt AB. FGF-21 as a novel metabolic regulator. J Clin Invest. 2005; 115:1627–1635. [PubMed: 15902306]

Kharitonenkov A, Wroblewski VJ, Koester A, Chen YF, Clutinger CK, Tigno XT, Hansen BC, Shanafelt AB, Etgen GJ. The metabolic state of diabetic monkeys is regulated by fibroblast growth factor-21. Endocrinology. 2007; 148:774–781. [PubMed: 17068132]

Kurosu H, Choi M, Ogawa Y, Dickson AS, Goetz R, Eliseenkova AV, Mohammadi M, Rosenblatt KP, Kliewer SA, Kuro-o M. Tissue-specific expression of betaKlotho and fibroblast growth factor (FGF) receptor isoforms determines metabolic activity of FGF19 and FGF21. J Biol Chem. 2007; 282:26687–26695. [PubMed: 17623664]

Lefterova MI, Zhang Y, Steger DJ, Schupp M, Schug J, Cristancho A, Feng D, Zhuo D, Stoeckert CJ Jr, Liu XS, Lazar MA. PPARgamma and C/EBP factors orchestrate adipocyte biology via adjacent binding on a genome-wide scale. Genes Dev. 2008; 22:2941–2952. [PubMed: 18981473]

Li K, Li L, Yang M, Zong H, Liu H, Yang G. Effects of rosiglitazone on fasting plasma fibroblast growth factor-21 levels in patients with type 2 diabetes mellitus. Eur J Endocrinol. 2009a; 161:391–395. [PubMed: 19528204]

Li X, Ge H, Weiszmann J, Hecht R, Li YS, Veniant MM, Xu J, Wu X, Lindberg R, Li Y. Inhibition of lipolysis may contribute to the acute regulation of plasma FFA and glucose by FGF21 in ob/ob mice. FEBS Lett. 2009b; 583:3230–3234. [PubMed: 19751733]

Lundasen T, Hunt MC, Nilsson LM, Sanyal S, Angelin B, Alexson SE, Rudling M. PPARalpha is a key regulator of hepatic FGF21. Biochem Biophys Res Commun. 2007; 360:437–440. [PubMed: 17601491]

Mai K, Andres J, Biedasek K, Weicht J, Bobbert T, Sabath M, Meinus S, Reinecke F, Mohlig M, Weickert MO, Clemenz M, Pfeiffer AF, Kintscher U, Spuler S, Spranger J. Free fatty acids link metabolism and regulation of the insulin-sensitizing fibroblast growth factor-21. Diabetes. 2009; 58:1532–1538. [PubMed: 19401423]

Moyers JS, Shiyanova TL, Mehrbod F, Dunbar JD, Noblitt TW, Otto KA, Reifel-Miller A, Kharitonenkov A. Molecular determinants of FGF-21 activity-synergy and cross-talk with PPARgamma signaling. J Cell Physiol. 2007; 210:1–6. [PubMed: 17063460]

Muise ES, Azzolina B, Kuo DW, El-Sherbeini M, Tan Y, Yuan X, Mu J, Thompson JR, Berger JP, Wong KK. Adipose fibroblast growth factor 21 is up-regulated by peroxisome proliferator-activated receptor gamma and altered metabolic states. Mol Pharmacol. 2008; 74:403–412. [PubMed: 18467542]

Ogawa Y, Kurosu H, Yamamoto M, Nandi A, Rosenblatt KP, Goetz R, Eliseenkova AV, Mohammadi M, Kuro-o M. BetaKlotho is required for metabolic activity of fibroblast growth factor 21. Proc Natl Acad Sci U S A. 2007; 104:7432–7437. [PubMed: 17452648]

Ohshima T, Koga H, Shimotohno K. Transcriptional activity of peroxisome proliferator-activated receptor gamma is modulated by SUMO-1 modification. J Biol Chem. 2004; 279:29551–29557. [PubMed: 15123625]

Pascual G, Fong AL, Ogawa S, Gamliel A, Li AC, Perissi V, Rose DW, Willson TM, Rosenfeld MG, Glass CK. A SUMOylation-dependent pathway mediates transrepression of inflammatory response genes by PPAR-gamma. Nature. 2005; 437:759–763. [PubMed: 16127449]

Potthoff MJ, Inagaki T, Satapati S, Ding X, He T, Goetz R, Mohammadi M, Finck BN, Mangelsdorf DJ, Kliewer SA, Burgess SC. FGF21 induces PGC-1alpha and regulates carbohydrate and fatty acid metabolism during the adaptive starvation response. Proc Natl Acad Sci U S A. 2009; 106:10853–10858. [PubMed: 19541642]

Reshef L, Olswang Y, Cassuto H, Blum B, Croniger CM, Kalhan SC, Tilghman SM, Hanson RW. Glyceroneogenesis and the triglyceride/fatty acid cycle. J Biol Chem. 2003; 278:30413–30416. [PubMed: 12788931]

Rosen ED, Sarraf P, Troy AE, Bradwin G, Moore K, Milstone DS, Spiegelman BM, Mortensen RM. PPAR gamma is required for the differentiation of adipose tissue in vivo and in vitro. Mol Cell. 1999; 4:611–617. [PubMed: 10549292]

Sarruf DA, Thaler JP, Morton GJ, German J, Fischer JD, Ogimoto K, Schwartz MW. Fibroblast growth factor 21 action in the brain increases energy expenditure and insulin sensitivity in obese rats. Diabetes. 2010; 59:1817–1824. [PubMed: 20357365]

0S hao D, Rangwala SM, Bailey ST, Krakow SL, Reginato MJ, Lazar MA. Interdomain communication regulating ligand binding by PPAR-gamma. Nature. 1998; 396:377–380. [PubMed: 9845075]

Spiegelman BM, Flier JS. Obesity and the regulation of energy balance. Cell. 2001; 104:531–543. [PubMed: 11239410]

Suzuki M, Uehara Y, Motomura-Matsuzaka K, Oki J, Koyama Y, Kimura M, Asada M, Komi-Kuramochi A, Oka S, Imamura T. betaKlotho is required for fibroblast growth factor (FGF) 21 signaling through FGF receptor (FGFR) 1c and FGFR3c. Mol Endocrinol. 2008; 22:1006–1014. [PubMed: 18187602]

Tontonoz P, Hu E, Graves RA, Budavari AI, Spiegelman BM. mPPAR gamma 2: tissue-specific regulator of an adipocyte enhancer. Genes Dev. 1994a; 8:1224–1234. [PubMed: 7926726]

Tontonoz P, Hu E, Spiegelman BM. Stimulation of adipogenesis in fibroblasts by PPAR gamma 2, a lipid-activated transcription factor. Cell. 1994b; 79:1147–1156. [PubMed: 8001151]

Tontonoz P, Spiegelman BM. Fat and beyond: the diverse biology of PPARgamma. Annu Rev Biochem. 2008; 77:289–312. [PubMed: 18518822]

Wang H, Qiang L, Farmer SR. Identification of a domain within peroxisome proliferator-activated receptor gamma regulating expression of a group of genes containing fibroblast growth factor 21 that are selectively repressed by SIRT1 in adipocytes. Mol Cell Biol. 2008; 28:188–200. [PubMed: 17954559]

Wente W, Efanov AM, Brenner M, Kharitonenkov A, Koster A, Sandusky GE, Sewing S, Treinies I, Zitzer H, Gromada J. Fibroblast growth factor-21 improves pancreatic beta-cell function and survival by activation of extracellular signal-regulated kinase 1/2 and Akt signaling pathways. Diabetes. 2006; 55:2470–2478. [PubMed: 16936195]

Willson TM, Lambert MH, Kliewer SA. Peroxisome proliferator-activated receptor gamma and metabolic disease. Annu Rev Biochem. 2001; 70:341–367. [PubMed: 11395411]

Wu Z, Bucher NL, Farmer SR. Induction of peroxisome proliferator-activated receptor gamma during the conversion of 3T3 fibroblasts into adipocytes is mediated by C/EBPbeta, C/EBPdelta, and glucocorticoids. Mol Cell Biol. 1996; 16:4128–4136. [PubMed: 8754811]

Wu Z, Rosen ED, Brun R, Hauser S, Adelmant G, Troy AE, McKeon C, Darlington GJ, Spiegelman BM. Cross-regulation of C/EBP alpha and PPAR gamma controls the transcriptional pathway of adipogenesis and insulin sensitivity. Mol Cell. 1999; 3:151–158. [PubMed: 10078198]

Wu Z, Xie Y, Bucher NL, Farmer SR. Conditional ectopic expression of C/EBP beta in NIH-3T3 cells induces PPAR gamma and stimulates adipogenesis. Genes Dev. 1995; 9:2350–2363. [PubMed: 7557387]

Wu Z, Xie Y, Morrison RF, Bucher NL, Farmer SR. PPARgamma induces the insulin-dependent glucose transporter GLUT4 in the absence of C/EBPalpha during the conversion of 3T3 fibroblasts into adipocytes. J Clin Invest. 1998; 101:22–32. [PubMed: 9421462]

Xu J, Lloyd DJ, Hale C, Stanislaus S, Chen M, Sivits G, Vonderfecht S, Hecht R, Li YS, Lindberg RA, Chen JL, Jung DY, Zhang Z, Ko HJ, Kim JK, Veniant MM. Fibroblast growth factor 21 reverses hepatic steatosis, increases energy expenditure, and improves insulin sensitivity in diet-induced obese mice. Diabetes. 2009; 58:250–259. [PubMed: 18840786]

Yamashita D, Yamaguchi T, Shimizu M, Nakata N, Hirose F, Osumi T. The transactivating function of peroxisome proliferator-activated receptor gamma is negatively regulated by SUMO conjugation in the amino-terminal domain. Genes Cells. 2004; 9:1017–1029. [PubMed: 15507114]

Yeh WC, Cao Z, Classon M, McKnight SL. Cascade regulation of terminal adipocyte differentiation by three members of the C/EBP family of leucine zipper proteins. Genes Dev. 1995; 9:168–181. [PubMed: 7531665]

Zhang H, Zhang A, Kohan DE, Nelson RD, Gonzalez FJ, Yang T. Collecting duct-specific deletion of peroxisome proliferator-activated receptor gamma blocks thiazolidinedione-induced fluid retention. Proc Natl Acad Sci U S A. 2005; 102:9406–9411. [PubMed: 15956187]

Zhang X, Yeung DC, Karpisek M, Stejskal D, Zhou ZG, Liu F, Wong RL, Chow WS, Tso AW, Lam KS, Xu A. Serum FGF21 levels are increased in obesity and are independently associated with the metabolic syndrome in humans. Diabetes. 2008; 57:1246–1253. [PubMed: 18252893]

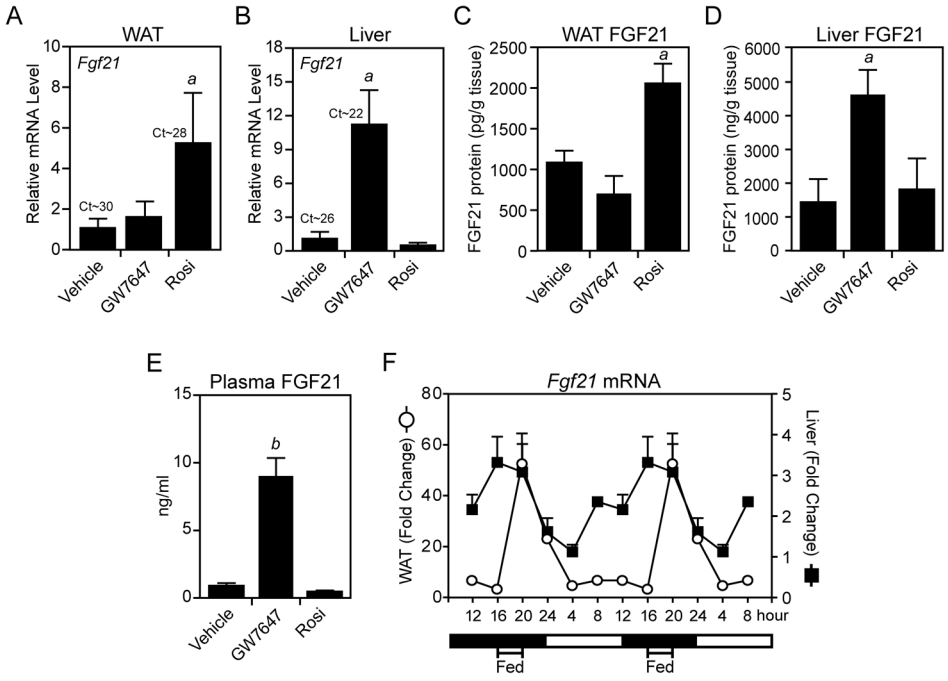

Figure 1. FGF21 is differentially regulated by PPARα and PPARγ agonists

(A–E) Two-month-old, male C57Bl/6 mice fed regular chow were treated for 17 hours with GW7647 (10 mg/kg), rosiglitazone (rosi; 10 mg/kg) or vehicle (1% methycellulose). *Fgf21* mRNA in epididymal (e) WAT **(A)** and liver **(B)** was measured by RT-qPCR. C_t values are indicated. FGF21 protein concentrations in eWAT **(C),** liver **(D)** and plasma **(E)** were measured by ELISA. For **(A–E)**, n=4/group. **(F)** Eight- to 10-week-old, male C57Bl/6 mice were food-entrained for 2 weeks by restricting their access to chow to a 4 hour period in the middle of the dark cycle. Tissues were collected at 4 hour intervals over a 24 hour period and *Fgf21* mRNA was analyzed by RT-qPCR. Data were normalized to *Fgf21* mRNA levels at their lowest point (16 hour for WAT, 4 hour for liver) and are double plotted (n=6/group). Error bars represent the mean ± SEM. *a*, $p<0.05$ vs vehicle; *b*, $p<0.01$ vs vehicle. See also Supplemental Figure S1.

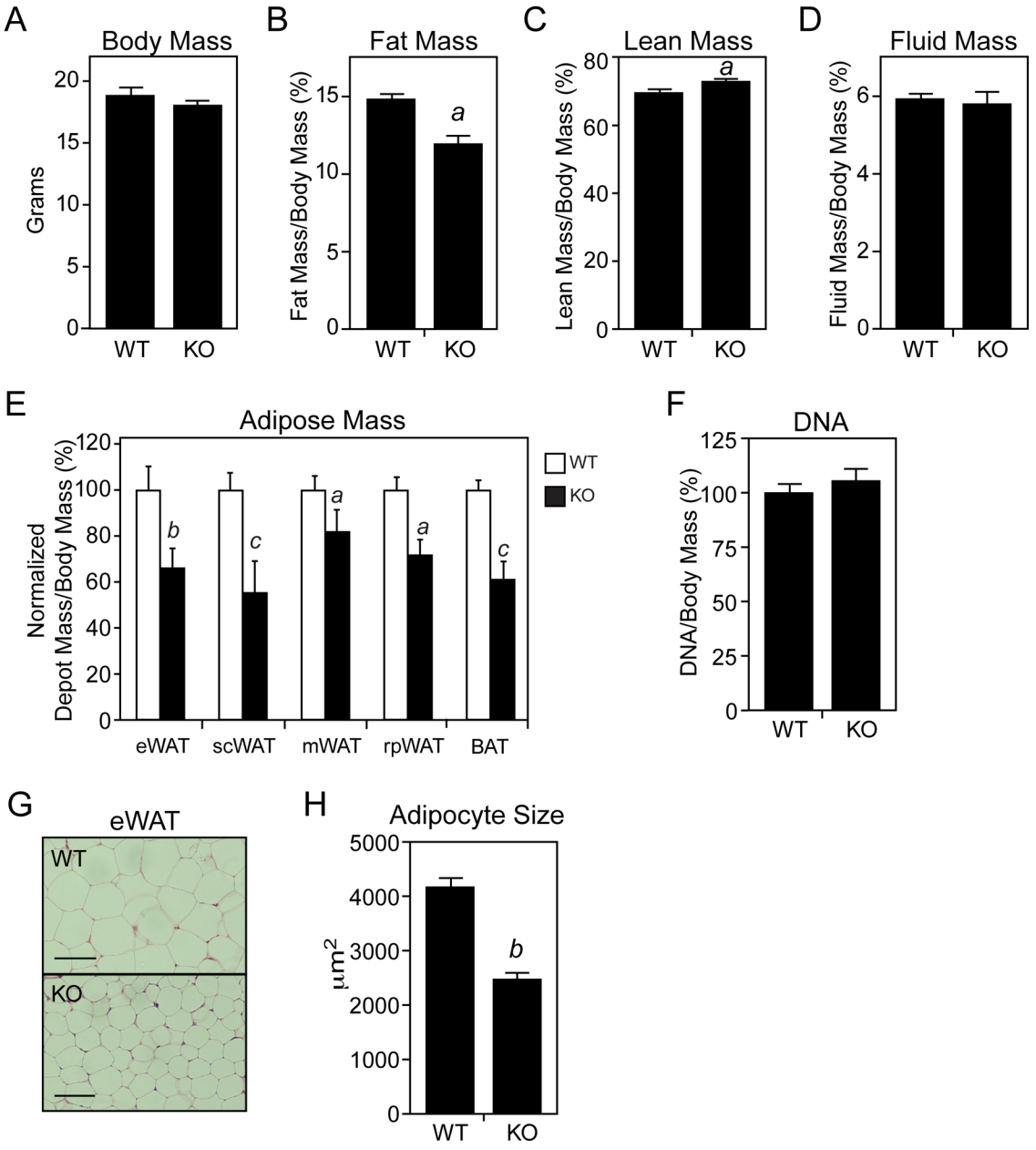

Figure 2. FGF21-knockout mice have decreased fat mass and adipocyte size

(A–E) The mass of various body depots was measured in 2-month-old, male wild-type (WT) and FGF21-knockout (KO) mice fed regular chow. For **(E)**, adipose tissue mass was measured and normalized to body weight for epididymal (e), subcutaneous (sc), mesenteric (m), retroperitoneal (rp) and brown adipose tissue (BAT) depots. For **(A–D)**, n=11–12/group; for **(E)**, n=6/group. **(F)** DNA content of eWAT pads was measured and normalized to body mass (n=4/group). **(G)** Representative hematoxylin and eosin-stained eWAT sections from WT and FGF21-KO mice. Scale bar = 100 μM. **(H)** Adipocyte size was measured using images of eWAT sections and ImageJ software (n>150 cells/group). Error bars represent the mean ± SEM. *a*, $p<0.05$ vs WT; *b*, $p<0.01$ vs WT; *c*, $p<0.005$. See also Supplemental Figure S2.

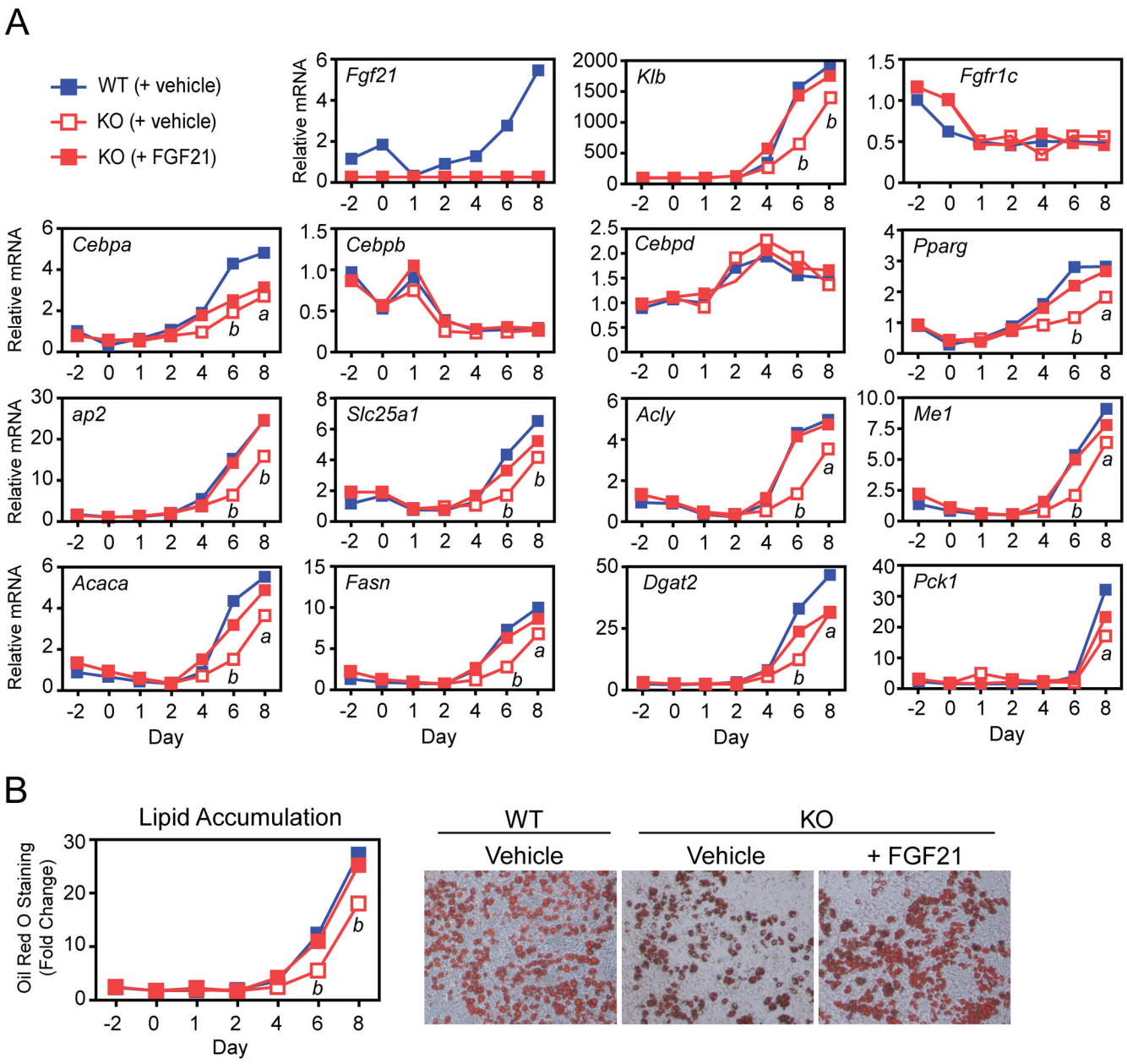

Figure 3. FGF21-knockout adipocytes have altered gene expression and lipid accumulation

(A, B) Stromal vascular fraction preadipocytes isolated from P4 wild-type (WT) and FGF21-knockout (KO) mice were differentiated in vitro over an 8 day period. FGF21-KO preadipocytes were differentiated in either the presence or absence of recombinant FGF21 (200 ng/ml). **(A)** Gene expression was measured by RT-qPCR. **(B)** Lipid accumulation was measured by oil red O staining. Representative oil red O-stained cells at day 8 of differentiation are shown. Error bars represent the mean ± SEM. *a*, $p<0.05$ vs WT; *b*, $p<0.01$ vs WT.

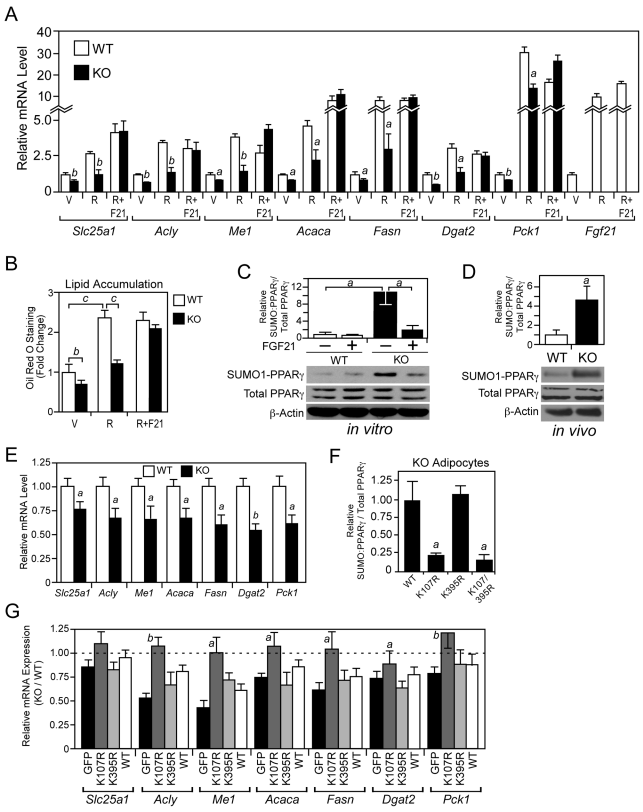

Figure 4. FGF21-knockout adipocytes have reduced PPARγ activity

(A–B) Stromal vascular fraction preadipocytes isolated from P4 wild-type (WT) and FGF21-knockout (KO) mice were differentiated for 8 days in the presence of 0.5 μM rosiglitazone (R), 0.5 μM rosiglitazone + 100 ng/ml FGF21 (R+F21) or vehicle (V). **(A)** Gene expression was measured by RT-qPCR. *a*, $p<0.05$ vs WT; *b*, $p<0.01$ vs WT. **(B)** Lipid accumulation was measured by oil red O staining. *b*, $p<0.01$; *c*, $p<0.005$. **(C)** Sumoylated and total PPARγ protein levels were measured in WT and FGF21-KO adipocytes differentiated for 8 days and treated with vehicle or FGF21 (200 ng/ml) for 4 hours prior to harvest. Sumoylated PPARγ was detected by immunoprecipitation with a SUMO1 antibody followed by western blot analysis with a PPARγ antibody. Phosphorylated and total PPARγ and β-actin were detected by western blot. Top panel, quantification by densitometry of sumoylated PPARγ normalized to total PPARγ is shown for an experiment performed in triplicate. *a*, $p<0.05$. Bottom panel, representative western blots are shown. **(D)** Sumoylated and total PPARγ protein levels were measured as in **(C)** in epididymal WAT extracts from 2- to 3-month-old male WT and FGF21-KO mice fed regular chow and killed in the fed state. Top panel, quantification by densitometry of sumoylated PPARγ normalized to total PPARγ for WT and KO mice (n=4/group). *a*, $p<0.05$. Bottom panel, western blots for pooled samples are shown. **(E)** Gene expression was measured by RT-qPCR in the epididymal WAT of 2- to 3-month-old, male WT and FGF21-KO mice killed during the fed state (n=6–7/group). *a*, $p<0.05$ vs WT; *b*, $p<0.01$ vs WT. **(F)** Flag-tagged PPARγ2, PPARγ2-K107R, PPARγ2-K395R or PPARγ2-K107R/K395R were introduced into primary FGF21-KO adipocytes by transfection and their sumoylation measured by immunoprecipitation with a Flag antibody followed by western blot analysis with either a SUMO1 or PPARγ antibody. Input levels of Flag-tagged PPARγ and the PPARγ mutants were determined by western blot analysis with a Flag antibody. Data were quantified by densitometry. *a*, $p<0.05$ vs WT. **(G)** Gene expression was measured by RT-qPCR in WT and

FGF21-KO stromal vascular fraction preadipocytes transduced with lentiviruses expressing PPARγ2, PPARγ2-K107R, PPARγ2-K395R or GFP control and differentiated for 4 days. PPARγ2, PPARγ2-K107R, PPARγ2-K395R were expressed at comparable levels (Figure S3E). Data are plotted as relative mRNA expression in FGF21-KO adipocytes compared to WT adipocytes. *a*, $p<0.05$ vs GFP; *b*, $p<0.01$ vs GFP. Error bars represent the mean ± SEM. See also Supplemental Figure S3.

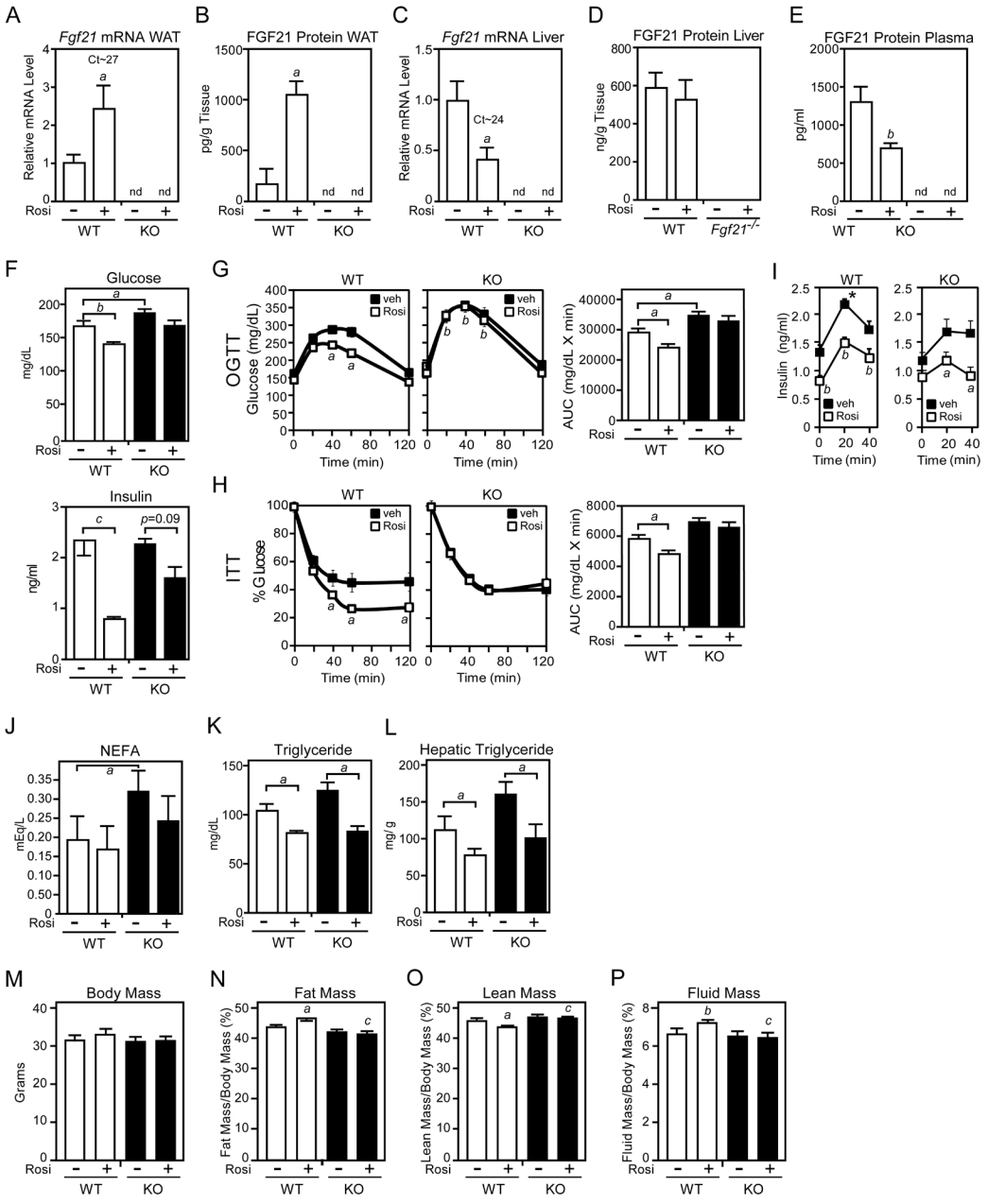

Figure 5. FGF21-knockout mice are refractory to rosiglitazone treatment

(A–P) Two- to 3-month-old male wild-type (WT) and FGF21-knockout (KO) mice were fed a high fat diet for 10 weeks. During the last two weeks, groups of mice were administered rosiglitazone (10 mg/kg) or vehicle (1% methylcellulose). The following parameters were measured: **(A)** *Fgf21* mRNA in epididymal WAT by RT-qPCR; **(B)** FGF21 protein in epididymal WAT by ELISA; **(C)** *Fgf21* mRNA in liver by RT-qPCR; **(D)** FGF21 protein in liver by ELISA; **(E)** Plasma FGF21 by ELISA; **(F)** Plasma glucose and insulin; **(G)** Plasma glucose concentrations for glucose tolerance tests in mice fasted for 8 hours; **(H)** Plasma glucose levels for insulin tolerance tests in mice fasted for 4 hours; **(I)** Plasma insulin concentrations during the glucose tolerance test; **(J)** Plasma non-esterified fatty acid concentrations; **(K)** Plasma triglyceride concentrations; **(L)** Hepatic triglyceride concentrations; **(M)** Body mass; **(N)** Fat mass; **(O)** Lean mass; **(P)** Fluid mass. For **(A–E)**,

n=5–6/group; for **(F–I)**, n=13–16/group; for **(J–P)**, n=5–6/group. For **(A–E)**, *a*, p<0.05 vs WT, vehicle; *b*, p<0.01 vs WT, vehicle; for **(F)**, *a*, p<0.05; *b*, p<0.01; *c*, p<0.005; for **(G)** and **(H)**, left panels, *a*, p<0.05 vs WT, vehicle; *b*, p<0.01 vs WT, vehicle; for **(G)** and **(H)**, right panels, *a*, p<0.05; for **(I)**, *a*, p<0.05 vs vehicle; *b*, p<0.01 vs vehicle; * p<0.05 vs FGF21-KO; for **(J–L)**, *a,* p<0.05; for **(N–P)** *a,* p<0.05 versus WT, vehicle; *b,* p<0.01 versus WT, vehicle; *c,* p<0.05 versus WT, rosiglitazone. Error bars represent the mean ± SEM. See also Supplemental Figure S4.

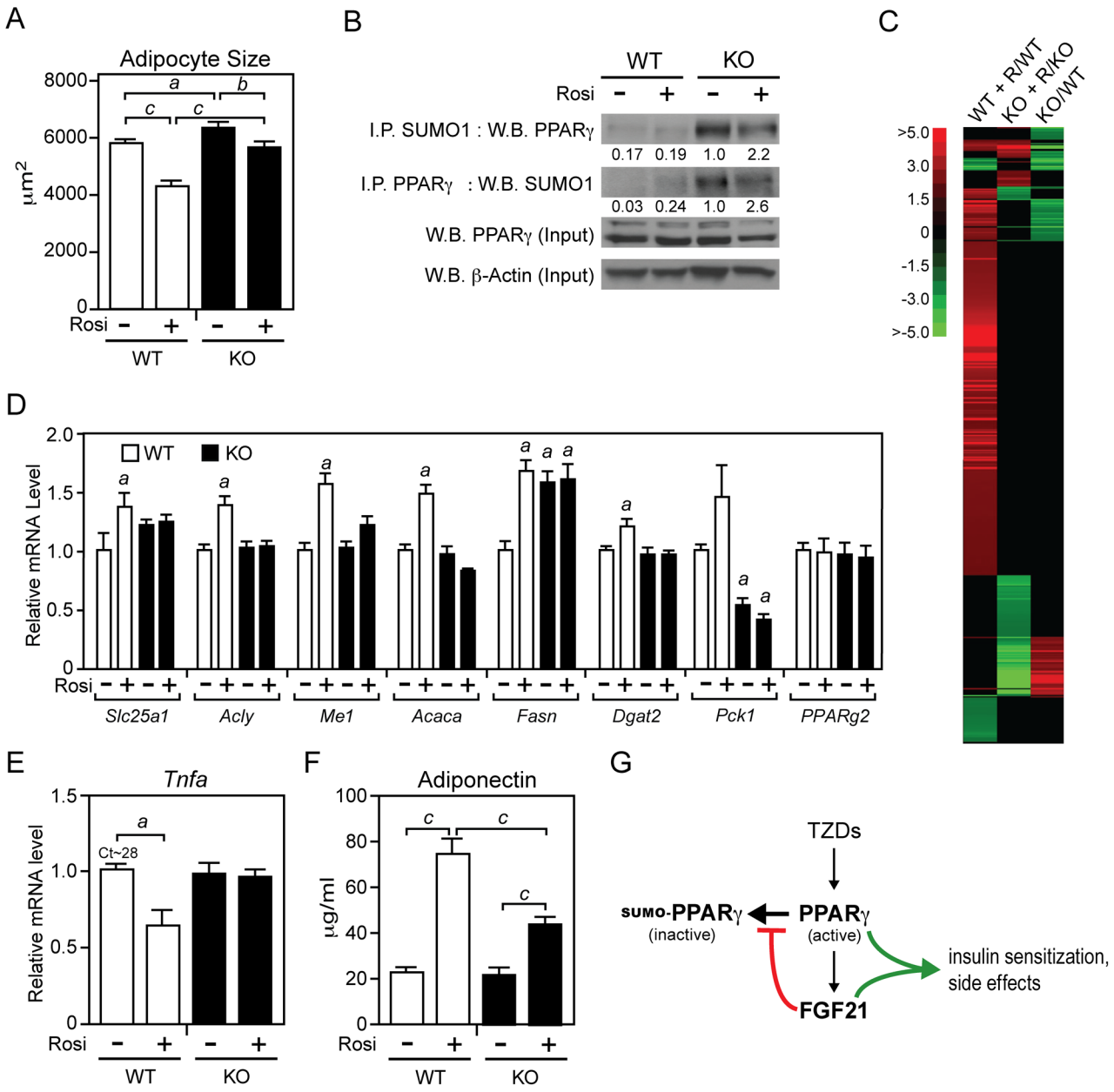

Figure 6. FGF21 is required for rosiglitazone effects in WAT

(A–E) Two- to 3-month-old wild-type (WT) and FGF21-knockout (KO) mice were fed a high fat diet for 10 weeks. During the last two weeks, groups of mice were administered rosiglitazone (10 mg/kg) or vehicle (1% methylcellulose). The following parameters were measured in epididymal WAT: **(A)** Adipocyte size was determined using ImageJ software (n>250 cells/group). *a,* p<0.05; *b,* p<0.01; *c,* p<0.001. **(B)** Sumoylated PPARγ was detected in epididymal WAT extracts by either immunoprecipitation with a SUMO1 antibody followed by western blot analysis with a PPARγ antibody or the reverse. Total PPARγ and β-actin were measured by western blot analysis. For each lane, WAT extracts were pooled from 4 mice. Numbers represent relative levels quantified by densitometry. **(C)** Microarray analysis resulted in the identification of 545 genes that were significantly changed in response to rosiglitazone treatment in epididymal WAT from either wild-type or FGF21-KO

mice. A heat map of the data is shown. R, rosiglitazone. **(D)** Gene expression was measured by RT-qPCR (n=5–6/group). *a*, $p<0.05$ versus WT, vehicle. **(E)** *Tnfa* mRNA was measured by RT-qPCR (n=5–6/group). *a*, $p<0.05$ versus WT, vehicle. **(F)** Plasma adiponectin concentrations were measured by ELISA (n=11–14/group). *c,* $p<0.001$. Error bars represent the mean ± SEM. **(G)** Model of the PPARγ-FGF21 regulatory pathway in adipose tissue. See also Supplemental Figure S5.